Electronic Supplementary Material (ESI) for New Journal of Chemistry.
This journal is © The Royal Society of Chemistry and the Centre National de la Recherche Scientifique 2021

Supporting Information

Preferential adsorption of ethane over ethylene on a Zr-based metal-organic framework: impacts of C-H···N hydrogen bond

Yaping Zhang,[a] Daofei Lv,[*b] Jiayu Chen,[c] Zewei Liu,[*c] Chongxiong Duan,[d] Xin Chen,[b] Wenbing Yuan,[b] Hongxia Xi[c] and Qibin Xia[c]

[a]*College of Harbour and Environmental Engineering, Jimei University, Xiamen 361021, PR China*

[b]*School of Environmental and Chemical Engineering, Foshan University, Foshan 528000, PR China*

[c]*School of Chemistry and Chemical Engineering, South China University of Technology, Guangzhou 510641, PR China*

[d]*School of Materials Science and Hydrogen Engineering, Foshan University, Foshan 528231, PR China*

Address correspondence to E-mail: lvdaofei@163.com (DL) and liuzeweiscut@gmail.com (ZL)

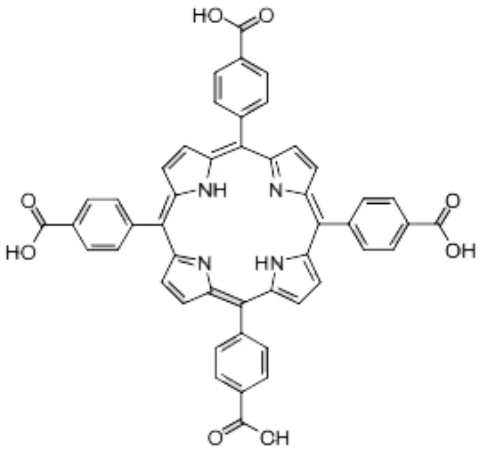

Fig. S1 The structure of tetrakis(4-carboxyphenyl)porphyrin (TCPP).

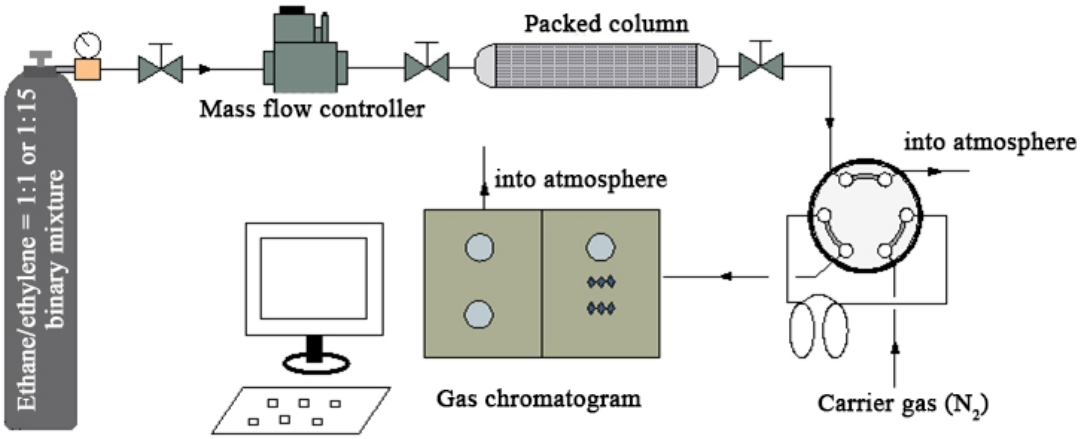

Fig. S2 Schematic illustration of the breakthrough experiments device.

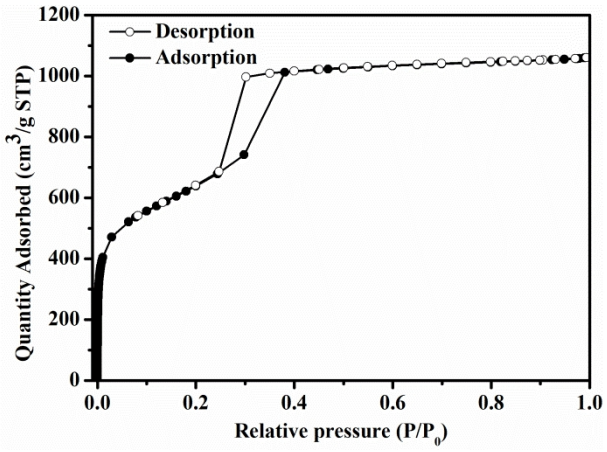

Fig. S3 N_2 adsorption/desorption isotherms of MOF-545 at 77 K.

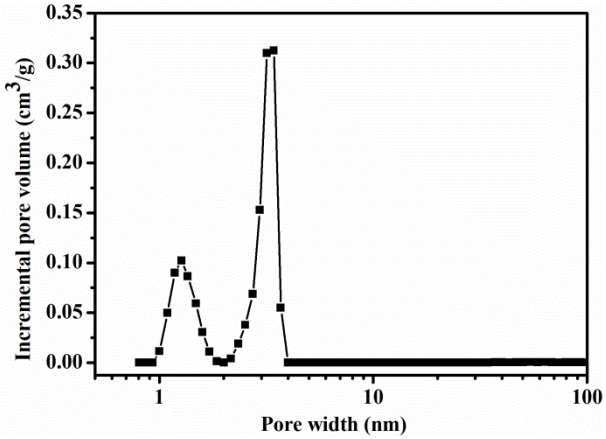

Fig. S4 Pore size distribution of MOF-545.

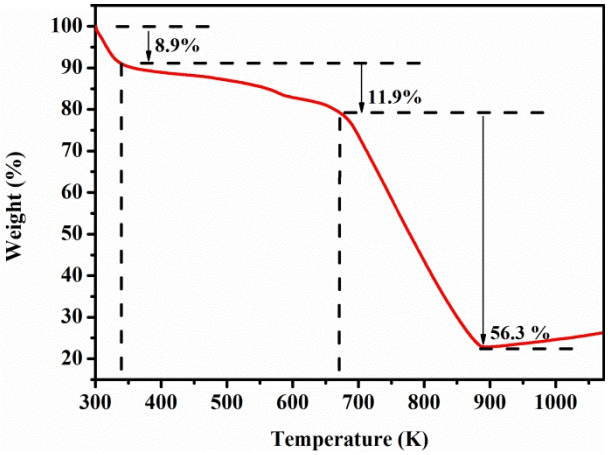

Fig. S5 TGA curve of MOF-545.

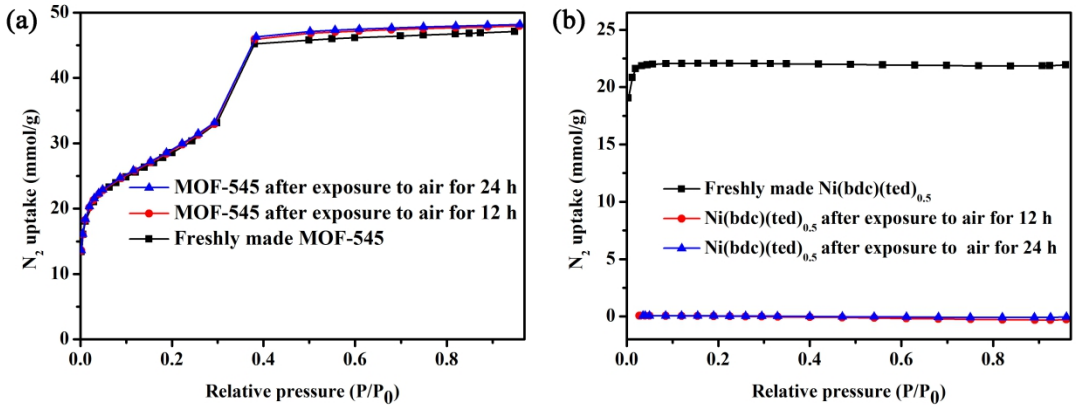

Fig. S6 N_2 sorption isotherms at 77 K of (a) MOF-545 and (b) Ni(bdc)(ted)$_{0.5}$ samples before and after exposure to air (43% RH) for 12 and 24 h.

Air stability

The stability experiments of samples under 43% relative humidity (RH) atmosphere were conducted by putting ~80 mg samples in a sealed chamber containing saturated potassium carbonate solution[1] for 12 or 24 h at ambient temperature. After that, samples were dried for 6 h at 393 K under vacuum. The stability of samples was characterized by PXRD and N_2 sorption experiments at 77 K.

Table S1 BET surface areas of MOF-545 and Ni(bdc)(ted)$_{0.5}$ samples after different tests

Samples	BET surface areas (m^2/g)	Langmuir surface areas (m^2/g)
Freshly made MOF-545	2265.4	3124.7
MOF-545 after exposure to air for 12 h	2262.8	3156.8
MOF-545 after exposure to air for 24 h	2276.1	3176.7
Freshly made Ni(bdc)(ted)$_{0.5}$	1977.0	2133.4
Ni(bdc)(ted)$_{0.5}$ after exposure to air for 12 h	4.6	0.1
Ni(bdc)(ted)$_{0.5}$ after exposure to air for 24 h	4.4	0.5

Table S2 Ethane and ethylene uptakes and ethane/ethylene IAST selectivities at 100 kPa on the selected ethane-selective adsorbents

Adsorbents	T (K)	Ethane uptake (mmol/g)	Ethylene uptake (mmol/g)	Ethane/ethylene selectivity[a]	The ratio of ethane/ethylene uptake	Ref.
Activated carbon (Calgon Co.)	303	2.66	1.78	-	-	2
Activated carbon	298	2.52	2.19	1.2[b]	1.15	3
ZIF-7	298	1.98	1.92	2.45	1.03	4
ZIF-8	293	2.50	1.50	1.85[c]	1.67	5
ZJU-121a	296	4.91	3.29	2.74	1.49	6
UTSA-33a	296	2.73	2.62	-	1.04	7
ZIF-69	298	2.20	1.77	1.66	1.24	8
MIL-53(Al)-FA	308	3.7	3.58	1.2	1.03	9
CPM-233	298	7.45	6.52	1.64	1.14	10
IRMOF-8	298	4.00	3.20	1.75	1.25	11
MAF-49	298	1.73	1.70	2.7	1.02	12
Ni(bdc)(ted)$_{0.5}$	298	5.0	3.4	1.85	1.59	13
Ni(TMBDC)(DABCO)$_{0.5}$	298	5.44	5	1.99[d]	1.09	14

MIL-142A	298	3.8	2.9	1.5	1.31	[15]
UiO-66-2CF_3	298	0.88	0.5	2.54	1.76	[16]
Ni-4PyC	298	3.8	3.5	1.7	1.09	[17]
NIIC-20-Bu	298	2.5	1.4	15.4	1.79	[18]
$Cu(Qc)_2$	298	1.85	0.78	3.4	2.37	[19]
PCN-245	298	3.27	2.39	1.80	1.37	[20]
$Fe_2(O_2)$(dobdc)	298	3.03	1.90	4.4	1.59	[21]
Zr-bptc	298	3.26	3.08	1.4	1.04	[22]
MOF-545	298	3.12	2.57	1.31	1.21	This work

a: ethane/ethylene selectivity towards equimolar ethane/ethylene mixtures.

b: selectivity at 303 K.

c: selectivity calculated on the basis of Henry constant.

d: ethane/ethylene selectivity towards ethane/ethylene = 1:15 mixtures.

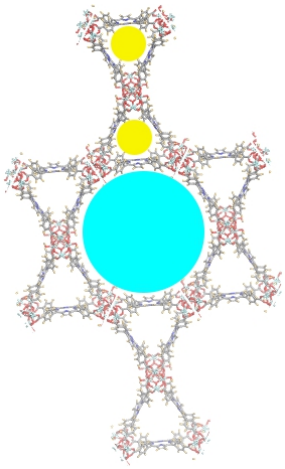

Fig. S7 The framework of MOF-545. The yellow and cobalt balls represent the small and large pores MOF-545, respectively.

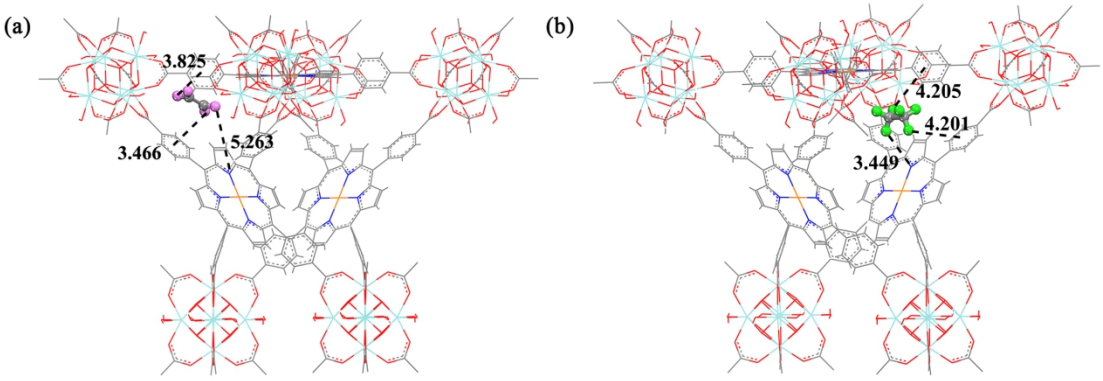

Fig. S8 The preferential binding sites of (a) ethylene and (b) ethane in MOF-545(Fe). Color code: N (blue), O (red), C (gray), H of ethylene (pink), H of ethane (cyan), Fe (orange) and Zr (light green).

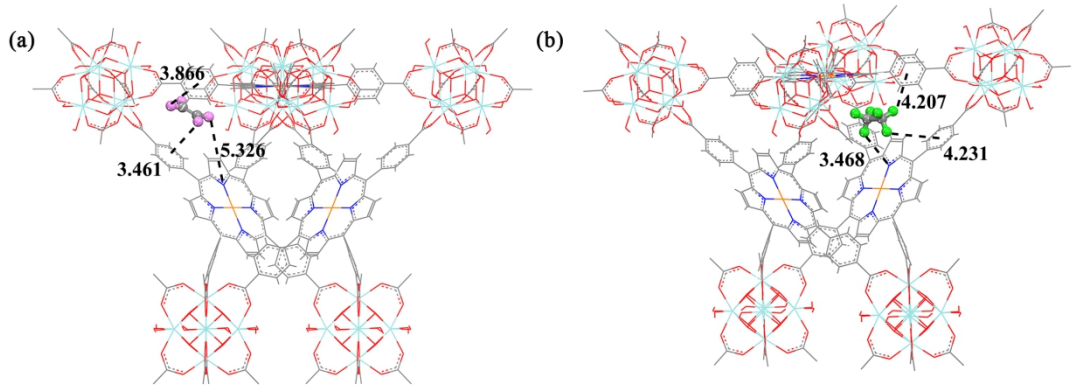

Fig. S9 The preferential binding sites of (a) ethylene and (b) ethane in MOF-545(Co). Color code: N (blue), O (red), C (gray), H of ethylene (pink), H of ethane (cyan), Co (orange) and Zr (light green).

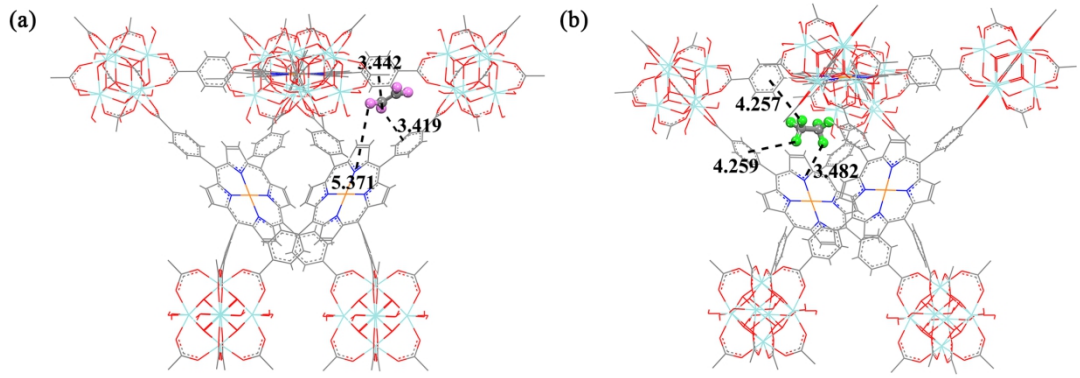

Fig. S10 The preferential binding sites of (a) ethylene and (b) ethane in MOF-545(Ni). Color code: N (blue), O (red), C (gray), H of ethylene (pink), H of ethane (cyan), Ni (orange) and Zr (light green).

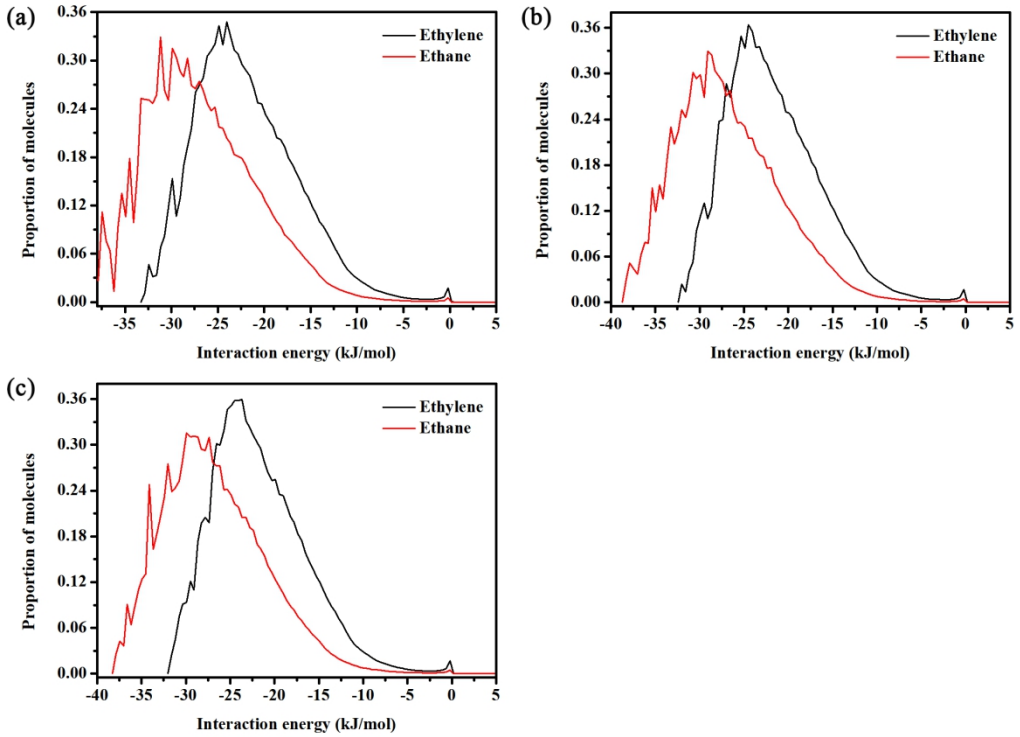

Fig. S11 The interaction energy distributions of ethane and ethylene in the frameworks of MOF-545(Fe) (a), MOF-545(Co) (b), and MOF-545(Ni) (c).

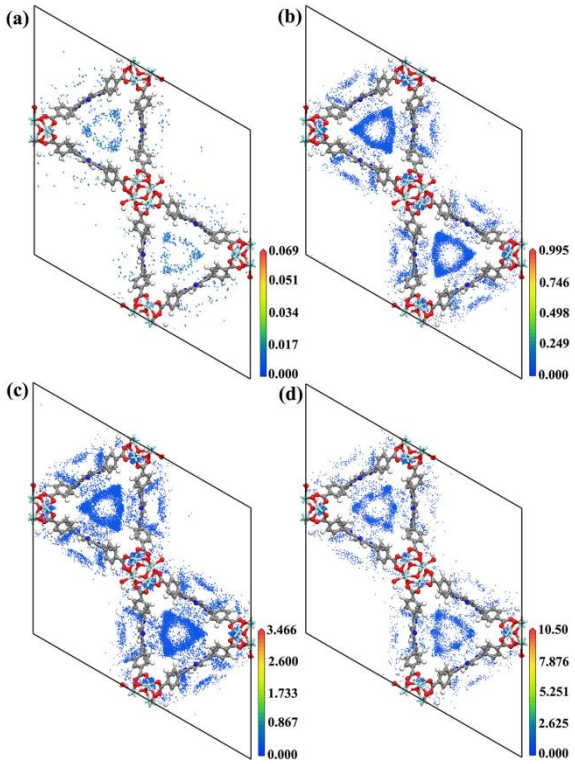

Fig. S12 Adsorption density contours of ethylene in MOF-545 at (a) 0.1 kPa; (b) 10 kPa; (c) 30 kPa and (d) 70 kPa. Color code: N (blue), O (red), C (gray), H (white) and Zr (light green).

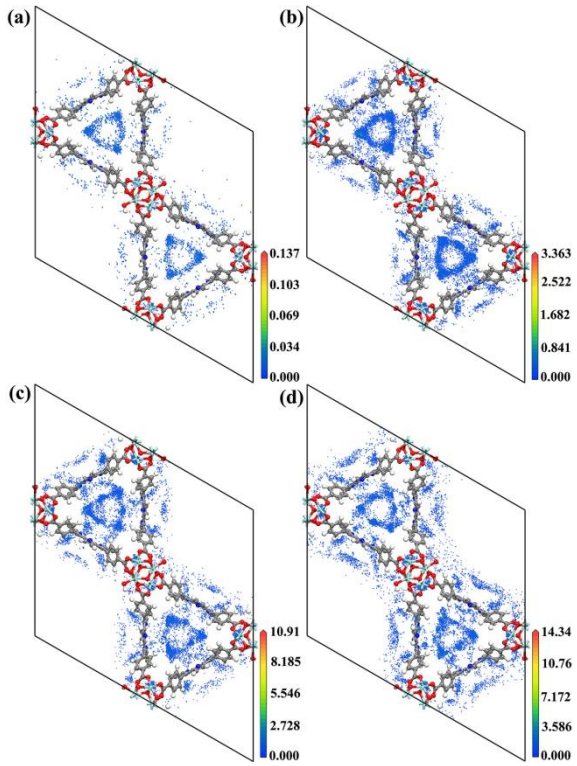

Fig. S13 Adsorption density contours of ethane in MOF-545 at (a) 0.1 kPa; (b) 10 kPa; (c) 30 kPa and (d) 70 kPa. Color code: N (blue), O (red), C (gray), H (white) and Zr (light green).

The calculation of Q_{st} based on Virial equation

Virial equation (Eq. S1) was used to fit ethane and ethylene sorption isotherms at 288, 298 and 308 K. After that, the fitting parameters were employed to calculate Q_{st} of ethane and ethylene utilizing Eq. S2.

$$\ln P = \ln N + \frac{1}{T}\sum_{i=0}^{m} a_i N^i + \sum_{i=0}^{n} b_i N^i \quad (1)$$

$$Q_{st} = -R\sum_{i=0}^{m} a_i N^i \quad (2)$$

where P represents pressure (mmHg), N refers to adsorption uptake (mg/g), T represents temperature (K), m and n are the number of coefficients required to well fit the sorption isotherms (herein, m = 8, n = 3), a_i and b_i represents Virial coefficients, and R refers to gas constant [J/(K· mol)].

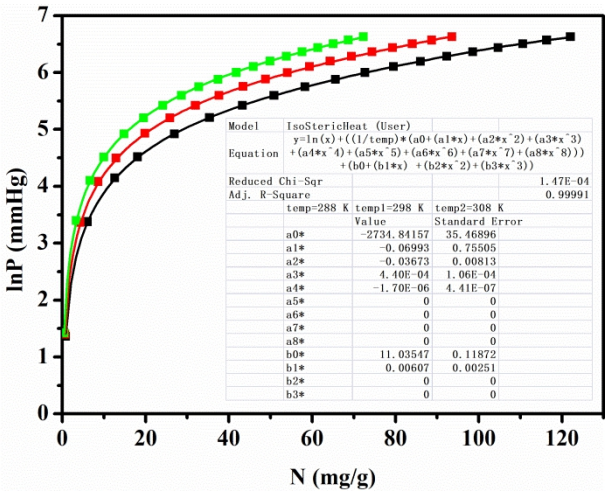

Fig. S14 Virial fitting (lines) of ethane adsorption isotherms (points) of MOF-545 measured at 288 (black), 298 (red), 308 (green) K. The inset shows the fittings of adsorption heat parameters of ethane adsorption in MOF-545.

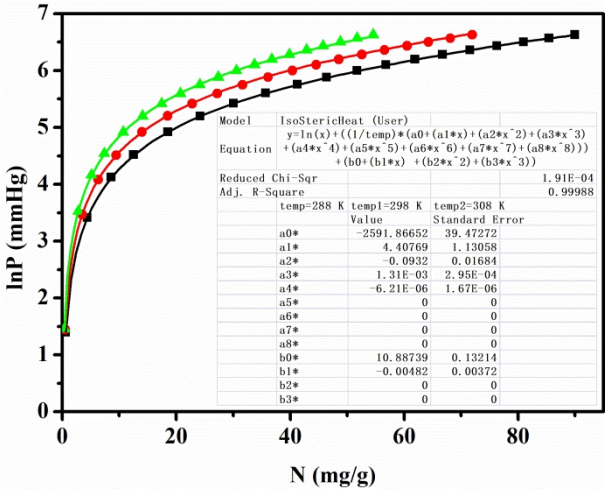

Fig. S15 Virial fitting (lines) of ethylene adsorption isotherms (points) of MOF-545 measured at 288 (black), 298 (red), 308 (green) K. The inset shows the fittings of adsorption heat parameters of ethylene adsorption in MOF-545.

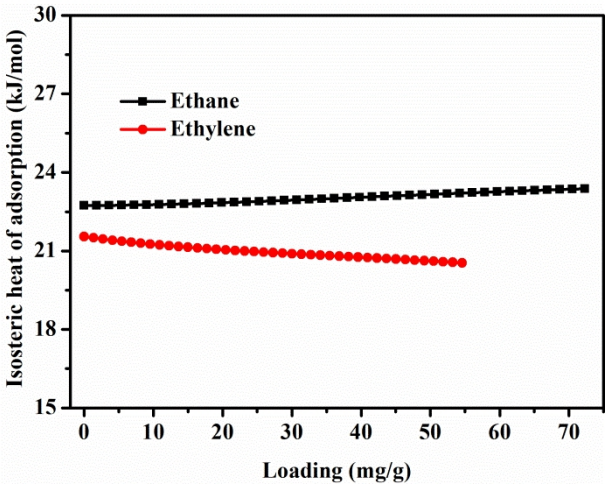

Fig. S16 The calculated isosteric heats of ethane and ethylene adsorption on MOF-545 on the basis of Virial equation.

Table S3 The fitting parameters of DSLF model for MOF-545

Gas	T/K	$q_{A,sat}$	k_A	m	$q_{B,sat}$	k_B	n	R^2
Ethylene	288	5.3843	6.5300E-3	0.9887	2.9802	2.7093E-4	1.6773	0.9999
	298	3.8434	2.8436E-4	1.6974	1.8662	1.8140E-2	0.8821	0.9999
	308	3.0925	1.7977E-4	1.7998	0.8992	2.5130E-2	1.0062	0.9999
Ethane	288	6.7652	6.6400E-3	0.9910	4.0123	7.4778E-4	1.4320	0.9999
	298	5.1023	2.2453E-4	1.6446	2.7973	1.3290E-2	0.9893	0.9999
	308	3.5344	4.0100E-4	1.6406	1.4927	2.1360E-2	0.9004	0.9999

The calculation of Q_{st} based on the combination of DSLF model and Clausius-Clapeyron equation

The isosteric heats of ethane and ethylene were also calculated based on the combination of DSLF model and Clausius-Clapeyron equation.

The Clausius-Clapeyron equation[20] after integration can be expressed as follows:

$$\ln p = -\frac{Q_{st}}{RT} + C \tag{3}$$

where p is the pressure (kPa), Q_{st} is the isosteric heat of adsorption (kJ/mol), R is the ideal gas constant [J/(mol·K)], T is the temperature (K), and C is the integral constant.

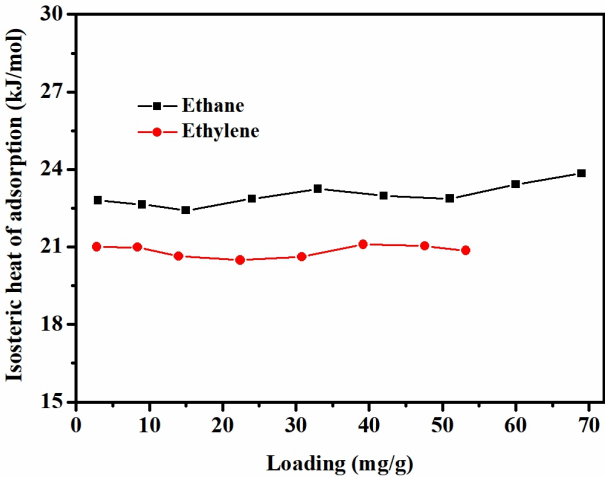

Fig. S17 The calculated isosteric heats of ethane and ethylene adsorption on MOF-545 on the basis of the combination of DSLF model and Clausius-Clapeyron equation.

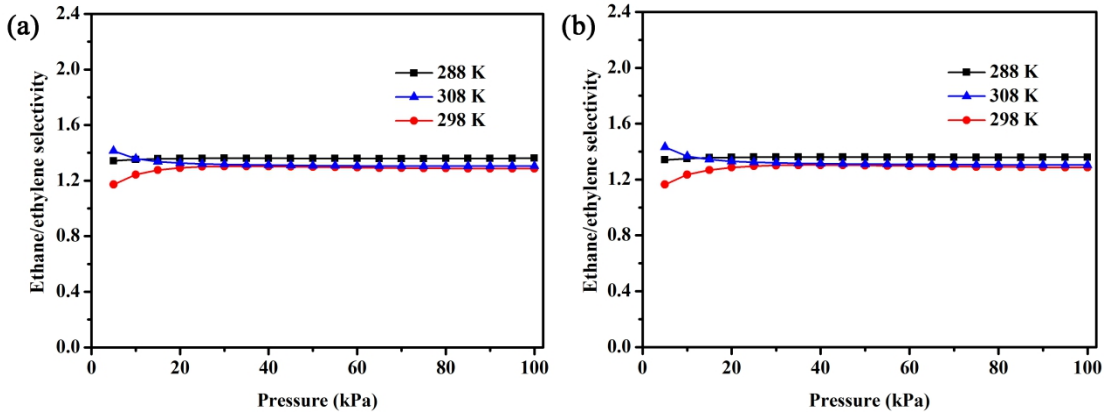

Fig. S18 IAST-predicted selectivities of ethane/ethylene binary mixtures on MOF-545 at 288, 298 and 308 K: (a) ethane/ethylene = 1:1 by volume; (b) ethane/ethylene = 1:15 by volume.

The calculation of ethane/ethylene selectivity for binary/ternary mixture on the basis of simulation calculations

Metropolis Monte Carlo method was used to calculate the adsorption density distribution of ethane, ethylene and typical impurities (methane, acetylene, propylene, or the trace amount of CO, CO_2, H_2S) in MOF-545. The force field models of typical impurities are obtained from the literatures[23-26]. To calculate ethane/ethylene selectivity for binary/ternary mixture, the molar ratio of C_2H_6 : C_2H_4 : CH_4 : C_2H_2 : C_3H_6 : CO : CO_2 : H_2S = 11.8% : 12.8% : 28.5% : 1% : 1.1% : 0.6% : 0.6% : 0.6% was used mostly with reference to the composition of refinery off-gas[27].

The ethane/ethylene selectivities were calculated according to the following

equation:

$$S_{ij} = \frac{x_i y_j}{x_j y_i}$$

where x_i and x_j are the ethane and ethylene uptakes on MOF-545, respectively, y_i and y_j are the mole fractions of ethane and ethylene, respectively.

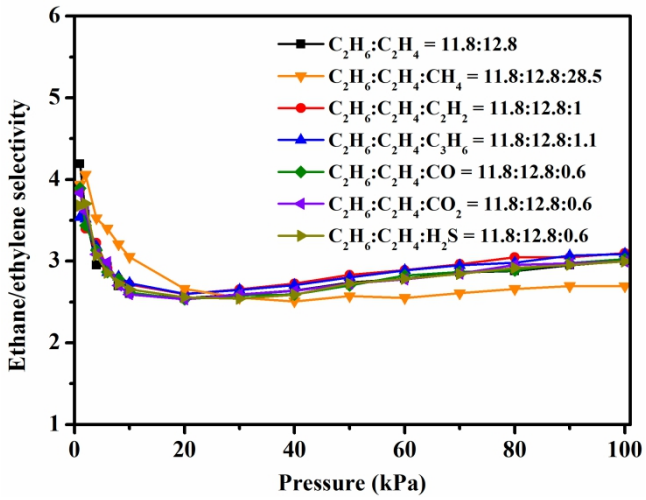

Fig. S19 Ethane/ethylene selectivity for binary/ternary mixture on MOF-545 at 298 K based on simulation calculations.

The calculation of simulated breakthrough curves of ethane/ethylene mixture on MOF-545 at ambient and high pressures

To obtain the breakthrough curves of ethane/ethylene mixture (ethane/ethylene = 1/15) at 1 and 35 bar (298 K) in a fixed-bed packed with adsorbent, the breakthrough curves of ethane/ethylene on MOF-545 were calculated. We assumed plug-flow conditions of the ethane/ethylene mixtures through a adsorption column with length of L = 1 m with the porosity of the column of 0.4 and the gas flow rate of 25 mL/min. Ethane and ethylene uptakes were assumed in the simulated breakthrough curves based on the fitting parameters of ethane/ethylene isotherms at 298 K. The concentration of ethane and ethylene can be expressed as follows:

$$\frac{\partial C_i}{\partial t} = -\frac{\partial (vC_i)}{\partial Z} - \left(\frac{1-\varepsilon}{\varepsilon}\right) RT\rho \frac{\partial q_i}{\partial t}$$

$$\frac{\partial C}{\partial t} = -\frac{\partial (vC)}{\partial Z} - \left(\frac{1-\varepsilon}{\varepsilon}\right) RT\rho \sum_{i=1}^{2} \frac{\partial q_i}{\partial t}$$

where t is the time, Z is the axial position along the fix-bed, v is the interstitial velocity, C_i is the concentration of component i, C is the total concentration of gas mixture, ε is the bed void fraction, ρ is the density of adsorbent, and q_i is the adsorbed amount for component i. v is calculated using Darcy's equation[28]:

$$\frac{\partial C}{\partial Z} = \frac{150\mu}{4(r_p)^2}\left(\frac{1-\varepsilon}{\varepsilon}\right)^2 v$$

where r_p is the particle radius, and μ is the fluid viscosity. q_i is calculated as following:

$$\frac{\partial q_i}{\partial t} = k_i(q_i^* - q_i)$$

where k_i is the mass-transfer coefficient for component i, and q_i* is the equilibrium uptake of component i. q_i* is calculated based on the single-component isotherm and IAST calculation.

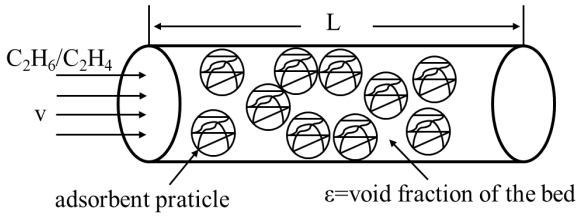

Fig. S20 Schematic diagram of simulated fixed bed.

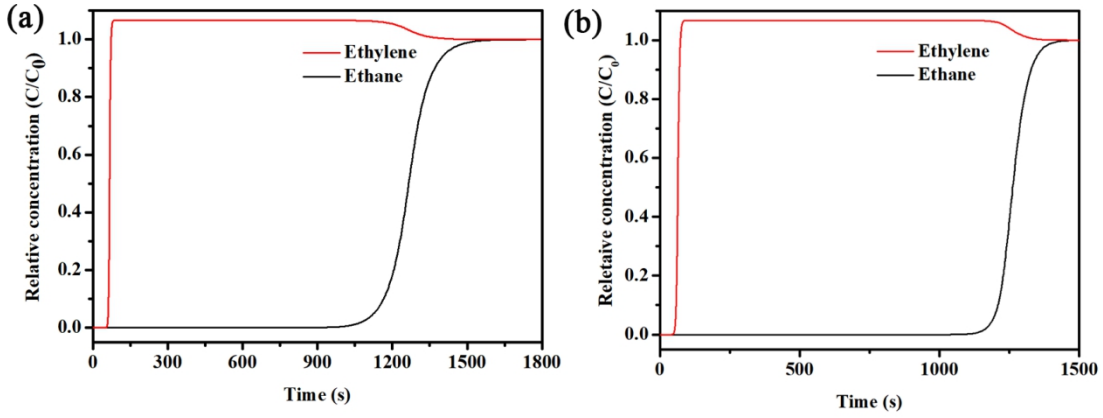

Fig. S21 Simulated breakthrough curves of ethane/ethylene mixtures (1:15 by volume) on MOF-545 at 298 K and different pressures: (a) 1 bar and (b) 35 bar.

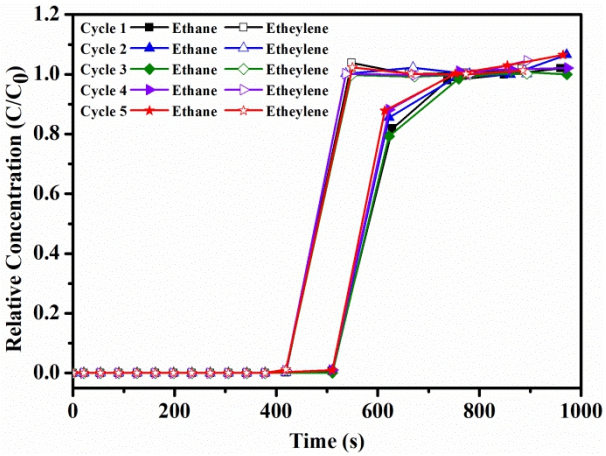

Fig. S22 Cyclic breakthrough curves for ethane/ethylene mixtures (1:15 by volume) on MOF-545 at 298 K and 100 kPa.

References

1 L. B. Rockland, *Anal. Chem.*, 1960, **32**, 1375-1376.

2 B. U. Choi, D. K. Choi, Y. W. Lee, B. K. Lee and S. H. Kim, *J. Chem. Eng. Data*, 2003, **48**, 603-607.

3 F. Gao, Y. Wang, X. Wang and S. Wang, *Adsorption*, 2016, **22**, 1-10.

4 D. L. Chen, N. Wang, C. Xu, G. Tu, W. Zhu and R. Krishna, *Microporous Mesoporous Mater.*, 2015, **208**, 55-65.

5 U. B?Hme, B. Barth, C. Paula, A. Kuhnt, W. Schwieger, A. Mundstock, J. Caro and M. Hartmann, *Langmuir*, 2013, **29**, 8592-8600.

6 J. Pei, J.-X. Wang, K. Shao, Y. Yang, Y. Cui, H. Wu, W. Zhou, B. Li and G. Qian, *J. Mater. Chem. A*, 2020, **8**, 3613-3620.

7 Y. He, Z. Zhang, S. Xiang, F. R. Fronczek, P. D. R. Krishna and P. D. B. Chen, *Chemistry*, 2012, **18**, 613-619.

8 W. Yuan, X. Zhang and L. Li, *J. Solid State Chem.*, 2017, **251**, 198-203.

9 J. Peng, Y. Sun, Y. Wu, Z. Lv and Z. Li, *Ind. Eng. Chem. Res.*, 2019, **58**, 8290-8295.

10 H. Yang, Y. Wang, R. Krishna, X. Jia, Y. Wang, A. N. Hong, C. Dang, H. E. Castillo, X. Bu and P. Feng, *J. Am. Chem. Soc.*, 2020, **142**, 2222-2227.

11 R. S. Pillai, M. L. Pinto, J. O. Pires, M. Jorge and J. R. B. Gomes, *ACS Appl. Mater. Interfaces*, 2015, **7**, 624-637.

12 P. Q. Liao, W. X. Zhang, J. P. Zhang and X. M. Chen, *Nat. Commun.*, 2015, **6**, 8697.

13 W. L. A, F. X. A, X. Z. A. B, J. X. B, Q. X. B, Y. L. A and Z. L. A, *Chem. Eng. Sci.*, 2016, **148**, 275-281.

14 X. Wang, Z. Niu, A. M. Al-Enizi, A. Nafady, Y. Wu, B. Aguila, G. Verma, L. Wojtas, Y. S. Chen and Z. Li, *J. Mater. Chem. A*, 2019, **7**, 13585-13590.

15 Y. Chen, H. Wu, D. Lv, R. Shi, Y. Chen, Q. Xia and Z. Li, *Ind. Eng. Chem. Res.*, 2018, **57**, 4063-4069.

16 J. Pires, J. Fernandes, K. Dedecker, J. R. B. Gomes, G. Pérez-Sánchez, F. Nouar, C. Serre and M. L. Pinto, *ACS Appl. Mater. Interfaces*, 2019, **11**, 27410-27421.

17 H. Wu, Y. Chen, W. Yang, D. Lv, Y. Yuan, Z. Qiao, H. Liang, Z. Li and Q. Xia, *Ind. Eng. Chem. Res.*, 2019, **58**, 10516-10523.

18 A. A. Lysova, D. G. Samsonenko, K. A. Kovalenko, A. S. Nizovtsev, D. N. Dybtsev and V. P. Fedin, *Angew. Chem. Int. Ed.*, 2020, **132**, 20742-20748.

19 R.-B. Lin, H. Wu, L. Li, X.-L. Tang, Z. Li, J. Gao, H. Cui, W. Zhou and B. Chen, *J. Am. Chem. Soc.*, 2018, **140**, 12940-12946.

20 D. Lv, R. Shi, Y. Chen, Y. Wu, H. Wu, H. Xi, Q. Xia and Z. Li, *ACS Appl. Mater. Interfaces*, 2018, **10**, 8366-8373.

21 L. Li, R.-B. Lin, R. Krishna, H. Li, S. Xiang, H. Wu, J. Li, W. Zhou and B. Chen, *Science*, 2018, **362**, 443-446.

22 D. Lv, J. Chen, Y. Chen, Z. Liu, Y. Xu, C. Duan, H. Wu, Y. Wu, J. Xiao, H. Xi, Z. Li and Q. Xia, *AIChE J.*, 2019, **65**, e16616.

23 J. R. Karra and K. S. Walton, *J. Phys. Chem. C*, 2010, **114**, 15735-15740.

24 G. Kamath, N. Lubna and J. J. Potoff, *J. Chem. Phys.*, 2005, **123**, 124505.

25 M. Fischer, F. Hoffmann and M. Fröba, *ChemPhysChem*, 2010, **11**, 2220-2229.

26 M. G. Martin and J. I. Siepmann, *J. Phys. Chem. B*, 1998, **102**, 2569-2577.

27 G. Jing, W. Xianghong, J. Shuhong, Q. Zhang and D. Zheng, *Chinese J. Chem. Eng.*, 2011, **19**, 543-548.

28 Y. G. Chung, P. Bai, M. Haranczyk, K. T. Leperi, P. Li, H. Zhang, T. C. Wang, T. Duerinck, F. You and J. T. Hupp, *Chem. Mater.*, 2017, **29**, 6315-6328.